



Title	The early stage of morphological maturation of cortical GABAergic interneurons
Author(s)	Yamasaki, Emi
Citation	大阪大学, 2013, 博士論文
Version Type	VoR
URL	https://doi.org/10.18910/26146
rights	
Note	

The University of Osaka Institutional Knowledge Archive : OUKA

<https://ir.library.osaka-u.ac.jp/>

The University of Osaka

The early stage of
morphological maturation of cortical
GABAergic interneurons

(大脳皮質 GABA 作動性介在神経細胞の
形態的初期成熟過程)

Emi Yamasaki

Graduate School of Frontier Bioscience
Osaka University

June 2013

Table of contents

General introduction (~references) · · · · ·	3-7
Abstract · · · · ·	8
Introduction · · · · ·	9-10
Materials and Methods · · · · ·	11-15
Results · · · · ·	16-25
Discussion · · · · ·	26-31
References · · · · ·	32-35
General discussion (~references) · · · · ·	36-41
Acknowledgements · · · · ·	42
Bibliography · · · · ·	43

General introduction

Neurons soon after birth have bipolar shape and do not make synaptic contact with other neurons. A mature neuron also has a bipolar shape processes information (Arimura and Kaibuchi, 2007). One of them termed axon send information to other neurons, while the other, termed dendrite, receive information from other neurons. Whereas mature neurons have highly branched axon and dendrites, neurons soon after birth have a simple shape and migrate to the destined place that is different from their birthplace. (Lambert de Rouvroit and Goffinet, 2001; Tsai and Gleeson, 2005).

Though the development from the simple process of a migrating neuron to the complex process such as an axon or dendrites of mature neurons has been discussed for several years, how neurons develop still remains controversial. In previous studies, the neuronal morphology in developmental stage was observed in fixed preparations (Stensaas, 1967a,b; Hinds and Hinds, 1974, 1978; Wentworth and Hinds, 1978; Martinez et al., 1992; Wilcock et al., 2007) and dissociated culture of hippocampal neurons (Dotti et al., 1988; Goslin and Bunker, 1989). Observation of fixed samples suggested that the polarity of mature neurons derive from the basoapical polarity of neuroepithelial cells. By contrast, the results of in vitro studies suggested that the establishment of axon-dendrite polarity is mediated by non-polarized cells.

To overcome the limitations of observations of fixed in vivo samples and dissociated neurons, observation of the process of morphological maturation in neurons in developing in vivo-like condition is necessary.

In this thesis, I examined the process of morphological maturation

using GABAergic interneurons in cerebral cortex as a model since their generation and migration that follows have been well documented. (Tanaka et al., 2003) Cortical GABAergic interneurons are born in ganglionic eminences (GE) and tangentially migrate to the cerebral cortex (Tamamaki et al., 1997; Anderson et al., 1997). On arriving at the cortex, they execute multidirectional migration and eventually settle in the cortical plate (CP) (Hevner et al., 2004; Tanaka et al., 2003, 2006, 2009). Therefore, I predicted that GABAergic interneurons terminate migration at a time when almost arrive in the CP and start maturation, and observed the dynamics of GABAergic interneurons.

I found that labeled cells that began to accumulate in the CP exhibited a sea urchin-like shape and suddenly extended a long axon-like process during the period of embryonic day (E)18.5 -postnatal day (P)2.5. The sea urchin-like cells extended and retracted many processes.

Thus, these findings suggested that cortical GABAergic interneurons transiently assume a sea urchin-like non-polarized shape prior to axon initiation.

References for general introduction

Anderson SA, Eisenstat DD, Shi L, Rubenstein JL (1997) Interneuron migration from basal forebrain to neocortex: dependence on Dlx genes. *Science*. 278:474-476.

Arimura N, Kaibuchi K (2007) Abstract Neuronal polarity: from extracellular signals to intracellular mechanisms. *Nat Rev Neurosci*. 8:194-205.

Dotti CG, Sullivan CA, Banker GA (1988) The establishment of polarity by hippocampal neurons in culture. *J Neurosci*. 8:1454-1468.

Goslin K, Banker G (1989) Experimental observations on the development of polarity by hippocampal neurons in culture. *J Cell Biol*. 108:1507-1516.

Hevner RF, Daza RA, Englund C, Kohtz J, Fink A (2004) Postnatal shifts of interneuron position in the neocortex of normal and reeler mice: evidence for inward radial migration. *Neuroscience*. 124:605-618.

Hinds JW, Hinds PL (1974) Early ganglion cell differentiation in the mouse retina: an electron microscopic analysis utilizing serial sections. *Dev Biol*. 37:381-341.

Hinds JW, Hinds PL (1978) Early development of amacrine cells in the mouse retina: An electron microscopic, serial section analysis. *J Comp Neurol*. 179:277-300.

Lambert de Rouvroit C, Goffinet AM (2001) Neuronal migration. *Mech Dev*. 105:47-56.

Martínez S, Puelles L, Alvarado-Mallart RM (1992) Tangential neuronal migration in the avian tectum: cell type identification and mapping of regional

differences with quail/chick homotopic transplants. *Brain Res Dev Brain Res.* 66:153-163.

Stensaas LJ (1967a) The development of hippocampal and dorsolateral pallial regions of the cerebral hemisphere in fetal rabbits. I. Fifteen millimeter stage, spongioblast morphology. *J Comp Neurol.* 129:59-69.

Stensaas LJ (1967b) The development of hippocampal and dorsolateral pallial regions of the cerebral hemisphere in fetal rabbits. II. Twenty millimeter stage, neuroblast morphology. *J Comp Neurol.* 129:71-83.

Tanaka DH, Maekawa K, Yanagawa Y, Obata K, Murakami F (2006) Multidirectional and multizonal tangential migration of GABAergic interneurons in the developing cerebral cortex. *Development* 133:2167-2176.

Tanaka D, Nakaya Y, Yanagawa Y, Obata K, Murakami F (2003) Multimodal tangential migration of neocortical GABAergic neurons independent of GPI-anchored proteins. *Development* 130:5803-5813.

Tanaka DH, Yanagida M, Zhu Y, Mikami S, Nagasawa T, Miyazaki J, Yanagawa Y, Obata K, Murakami F (2009) Random walk behavior of migrating cortical interneurons in the marginal zone: time-lapse analysis in flat-mount cortex. *J. Neurosci.* 29:1300-1311.

Tamamaki N, Fujimori KE, Takaaji R (1997) Origin and route of tangentially migrating neurons in the developing neocortical intermediate zone. *J Neurosci* 17:8313-8323.

Tsai LH, Gleeson JG (2005) Nucleokinesis in neuronal migration. *Neuron* 46:383-388.

Wentworth LE, Hinds JW (1978) Early motoneuron formation in the cervical spinal cord of the mouse: an electron microscopic, serial section analysis. *J Comp*

Neurol. 177:611-613.

Wilcock AC, Swedlow JR, Storey KG (2007) Mitotic spindle orientation distinguishes stem cell and terminal modes of neuron production in the early spinal cord. *Development*. 134:1943-1954.

Abstract

Mature neurons polarize by extending an axon and dendrites. In vitro studies of dissociated neurons have demonstrated that axons are initiated from a non-polarized stage. Dissociated hippocampal neurons form four to five minor neurites shortly after plating but then one of them starts to elongate rapidly to become the future axon, whereas the rest constitutes the dendrites at later stages. However, neuroepithelial cells as well as migrating neurons *in vivo* are already polarized, raising the possibility that mature neurons inherit the polarities of immature neurons of neuroepithelial or migrating neurons. Here I show that the axon of interneurons in mouse cortical explant emerges from a morphologically non-polarized shape. The morphological maturation of cortical interneurons labeled by electroporation at an embryonic stage was analyzed by time-lapse imaging during the perinatal stage. In contrast to earlier stages, most interneurons at this stage show sea urchin-like non-polarized shapes with alternately extending and retracting short processes. Abruptly, one of these processes extends to give rise to an outstandingly long axon-like process. Given that the interneurons exhibit typical polarized shapes during embryonic development, the present results suggest that axon-dendrite polarity develops from a non-polarized intermediate stage.

Introduction

Neurons typically show polarized morphology, defined as a single axon and several dendrites. A fundamental question is how is this axon-dendrite polarity established. Although there is evidence that an extrinsic directional cue can induce axons (Adler et al., 2006), developing neurons can acquire polarity in culture in the absence of any extrinsic signal directional gradients (for review, see Arimura and Kaibuchi, 2007). This issue has been extensively studied using hippocampal cells in culture: these cells, shortly after plating, extend lamellipodia, which then develop into several short, immature neurites (Dotti et al., 1988; Goslin and Bunker, 1989). After a period of alternating elongation and retraction, one process acquires an axonal nature. Once a single process acquires the axonal nature, none of the remaining processes become an axon. These findings indicate that axon-dendrite polarity determination is an intrinsically regulated selection in which the “winner” among equivalent early processes becomes an axon.

However, most postmitotic neurons *in situ* are already polarized at the time of generation, because neuroepithelial cells have basoapical polarity. Thus, neurons that arise from neuroepithelial cells could in some way inherit basoapical polarity, which could then lead to the establishment of axon-dendritic polarity. This idea is supported by observations of early development of neurons in fixed preparations (Stensaas, 1967a,b; Hinds and Hinds, 1974, 1978; Wentworth and Hinds, 1978; Martínez et al., 1992; Wilcock et al., 2007) in which basal processes appear to turn into axons. Moreover, neurons or neuronal precursors that have just been separated from neuroepithelial cells by cell

division are also polarized with morphologies of migrating cells (Lambert de Rouvroit and Goffinet, 2001; Tsai and Gleeson, 2005), indicating that neurons are in some way already polarized *in vivo* before extending axons.

Nevertheless, the idea that axon-dendrite polarity emerges from a non-polarized stage *in vivo* cannot be ruled out, because there is insufficient literature on the sequential changes in morphology during the transformation of migrating neurons into axon-dendrite polarized mature ones in the developing brain. To address this issue, I focused on cortical interneurons because their generation occurs at a location different from that of maturation, which enables me to analyze the process of maturation separately from early neurogenesis. These neurons are generated in ganglionic eminences in the basal forebrain (Anderson et al., 1997; Tamamaki et al., 1997) and migrate to the neocortex. Previously, it is indicated that interneurons labeled by electroporation at E12.5 execute multidirectional tangential migration in the marginal zone (MZ) of the neocortex for a protracted period of time (Tanaka et al., 2003, 2006, 2009). During this period, many interneurons change their direction of migration by changing their polarity of migration (Tanaka et al., 2009). Thereafter, these neurons descend to the CP (Tanaka et al., 2009).

Here I performed long-time (>40 hrs) live imaging of cortical interneurons at the stage when they reach the CP by using organ culture preparations that recapitulate their *in vivo* development. I found that cortical interneurons transiently assume a non-polarized shape during early postnatal development alternately extending and retracting many short processes. One of these processes rapidly elongates far beyond the length of the alternating extensions and retractions, suggesting that polarity begins from non-polarized stage.

Materials and methods

Animals

ICR mice of both sexes were used in most of the experiments. GAD67-GFP (Δ neo) mice (Tamamaki et al., 2003) were used in some experiments in which interneurons were labeled by DsRed2. They were also used to confirm that the laminated structure of the cortex is retained in our culture condition. Noon on the day of vaginal plug detection was defined embryonic day (E) 0.5; E19.5 was defined as postnatal day (P) 0. All experiments were done in accordance with institutional guidelines.

Electroporation

In or *ex utero* electroporation into the medial ganglionic eminence (MGE) was performed on E12.5 embryos. Plasmid vectors used were *pCAGGS-DsRed2*, *pCAG-EGFP* and *pCAGGS-GAP-EGFP*. Unless otherwise stated, data shown in figures and movies were from cells labelled with *pCAGGS-GAP-EGFP* but essentially the same results were obtained when using *pCAGGS-DsRed2* (Movie 6). The methods for electroporation were similar to those described previously (Tanaka et al., 2006), except that 30-34V electric pulses were delivered at 800 msec intervals for *ex utero* electroporation and 60V-pulses at 600 msec intervals for *in utero* electroporation.

Staining and quantitative analysis of fixed samples

A mixture of *pCAG-EGFP* and *pCAGGS-GAP-EGFP* was electroporated as described above. E18.5 to P2.5 brains were dissected from electroporated mice

and immersion fixed in 4% paraformaldehyde (PFA) in phosphate buffer (PB) overnight at 4°C, cut coronally at 50 μ m on a vibrating-blade microtome, and stained with an anti-GFP antibody. P7-P21 mice were transcardially perfused with 4% PFA in PB under deep anesthesia with sodium pentobarbitone (Nembutal; 100-200 mg/kg body weight; Abbott Laboratories) before immersion fixation. Sections were sampled from the intermediate one-third of the neocortex along the rostrocaudal axis, extending caudally to the level of the caudal end of the hippocampus. The slices were transferred to 48-well plates and incubated in biotin-conjugated anti-GFP (1:500; Rockland Immunochemicals) in 0.3% Triton X-100/PBS for 2-6 d at 4°C, followed by 5 h incubation in Alexa Fluor 488 streptavidin (1:200; Invitrogen) at room temperature (RT). Then sections were counterstained with TO-PRO-3 iodide (1:2000; Invitrogen) at RT. The slices were then divided into three groups: rostral, intermediate, and caudal. A set of three consecutive sections was arbitrarily chosen from each of the group and was subjected to confocal microscopy (FV1000; Olympus). Confocal images taken from the three consecutive sections were superimposed by adjusting the tissue border. In some experiments, a motor-driven light microscope stage was used to capture images at multiple points in a wide field but with a high magnification. The images from each point were assembled thereafter. The following filter sets were used with the indicated wave lengths for excitation laser line and emission filters (in nm): GFP (green), 488/(505-525); TO-PRO-3 (far red), 633/(650) with FV1000. To identify the tissue border, DIC images were captured simultaneously with the fluorescent images. Adobe Photoshop 7.0 software was used for images processing described above.

For quantitative analysis, the second section in the triplet was picked up. Labeled cells were counted between the line drawn tangentially to the medial

surface of the lateral ventricle and the one drawn perpendicularly to the lateral surface of the cortex from the edge of the corticostriatal sulcus.

To assess the orientation of GABAergic neurons, a line was drawn from the center of the cell body to the tip of the longest process emanating from the cell body. Then, the length of this line and the angle between this line and a line drawn perpendicular to the pial surface at the point where the former intersects with the pial surface were measured. To define the center of the cell body, two lines were drawn tangentially to the cell body surface, each on its opposite side and parallel with each other, and the midpoint between the point of two tangency was defined as its center. When the angles (x) were $0^\circ < x < 45^\circ$, $135^\circ < x < 225^\circ$, $315^\circ < x < 360^\circ$, the direction was defined as radial. When the angles (x) were $45^\circ < x < 135^\circ$ and $225^\circ < x < 315^\circ$, the direction was defined as tangential. The layer distribution of labeled cells between the ventricular zone and the marginal zone of cerebral cortex was also examined by nuclear staining.

For immunostaining of axons with axonal markers, $50\ \mu\text{m}$ -thick sections were cut from a P2.5 mouse brain on a vibrating-blade microtome and reacted with a mixture of mouse anti-SMI-312 monoclonal antibody (1:1000; Covance) and goat biotin-conjugated anti-GFP (1:500; Rockland Immunochemicals) for at least 2 d at 4°C , washed with PBS, followed by a mixture of cyanine 3 (Cy3)-conjugated anti-mouse IgG (1:200; Jackson ImmunoResearch) and Alexa Fluor 488-streptavidin (1: 200; Invitrogen) for 4-6 h at RT. To determine transmitter phenotypes, P21 fixed brains were cryoprotected by immersion in 30% sucrose and cut coronally at $20\ \mu\text{m}$. The sections were mounted on slides and washed with PBS. The sections were then incubated in PBS with 0.5% Triton X-100 and 5-10% normal goat serum (NGS) for 2-5 h at RT. This was followed by incubation in the primary antibody diluted

in PBS with 0.5% Triton X-100 and 5% NGS for 2 d at RT. The primary antibodies used were as follows: rabbit anti-parvalbumin (PV) (1:2000 to 1:4000; Swant), rat anti-somatostatin (SST) (1:100; Millipore Bioscience Research Reagents, and rabbit anti-calretinin (CR) (1:2000; Swant). The sections were incubated for 3 h at RT in the secondary antibody diluted in 1% NGS in PBS with 0.5% Triton X-100. The secondary antibodies used were either goat Cy3-conjugated anti-rabbit IgG (1:100) or goat Cy3-conjugated anti-rat IgG (1:200) (both from Jackson ImmunoResearch). For nuclear staining, all sections were incubated in 0.03% 4,6-diamidino-2-phenylindole (Nacalai Tesque) in PBS for 30 min at RT. Images were captured using a CCD camera (AxioCam; Carl Zeiss) attached to an epifluorescence microscope (BX60; Olympus).

Time-lapse imaging

The head of E18.5 or P0.5 electroporated mice was removed and placed in a plastic dish filled with Hanks' solution with the dorsal surface of the brain exposed. Then the brain was chilled by placing the dish in a freezer (-20°C) for 5-10 min to slightly harden the brain. Brains were then cut into two halves at an intermediate level along the rostrocaudal axis in Hanks' solution (Nissui, TOKYO) on a vibrating-blade microtome (VT-1000; Leica Microsystems). The rostral half of the cut brain was mounted onto membrane inserts (Millicell-CM PICMORG50; Millipore) coated with collagen gels with the sectioned side down. The foot of the mounted tissue was covered with collagen gels and maintained in Opti-MEM I reduced-serum medium containing 2.5% heat-inactivated fetal bovine serum, 2.5% heat-inactivated horse serum, 1% N2 supplement (all from Invitrogen, Grand Island, NY), 20mM D-glucose and 20µg/ml streptomycin (Sigma). After culturing the hemisected brain for 4-6 hrs, the preparation was

transferred to a glass bottom dish (FluoroDish FD35-100; World Precision Instruments) in a temperature- and gas-controlled incubation chamber (5% CO₂, 95% O₂ at 37°C) fitted onto a confocal microscope (FV1000, OLYMPUS) that was equipped with a motor-driven X-Y stage (FC-101G, Sigma Koki).

Labeled cells were viewed through a 20X objective (N.A.=0.45). Images were collected with the confocal microscope using a 488 nm excitation wavelength and 505-525 nm emission filter for GFP or a 543 nm excitation wavelength and 560 nm emission filter for DsRed. Images were captured from multiple points of the cerebral cortex by moving a motor-driven X-Y stage regulated by the aid of multi-area time-lapse software (FV10-ASW ver1.6b, Olympus). Time-lapse imaging was carried out for 36-43 hrs at 30 minutes time intervals. At each time point, a stack of images was created from a series of 4-5 consecutive images taken along the z-axis at 10µm intervals. The tissue boundary was identified by referring to DIC images. The laminated structure of the cortex was retained during the course of imaging. Brightness and contrast were adjusted for every frame using Adobe Photoshop 7.0 or CS4 software. Movies were assembled using Adobe Photoshop CS4 or ImageReady 7.0 software.

Results

Sea urchin-like cells

Many cortical interneurons labeled by electroporation at E12.5 are observed in the MZ at E18.5 but become predominantly localized at the CP from P2 onward (Tanaka et al., 2009). This suggests that these interneurons begin to terminate migration and mature during E18.5 to P2. Therefore, I began time-lapse imaging at E18.5 or P0.5 and thereafter examined the dynamics of labeled cells in the CP.

A major population of labeled cells in the CP exhibited a multipolar morphology (Fig. 1A) and alternately extended and retracted numerous short processes (Fig. 1 A-C), although rapidly migrating cells extending a leading process were also observed. Such multipolar cells did not substantially change the position of their cell body (Fig. 1 A, B), unlike those with a simple bipolar morphology observed at earlier stages (Tanaka et al., 2003, 2006, 2009). This suggests that these cells are nearing the completion of their migration, in agreement with a previous report that found cortical interneurons lose motility during the early postnatal stage (Bortone and Polleux, 2009). Because of their peculiar features, I termed such cells sea urchin-like cells.

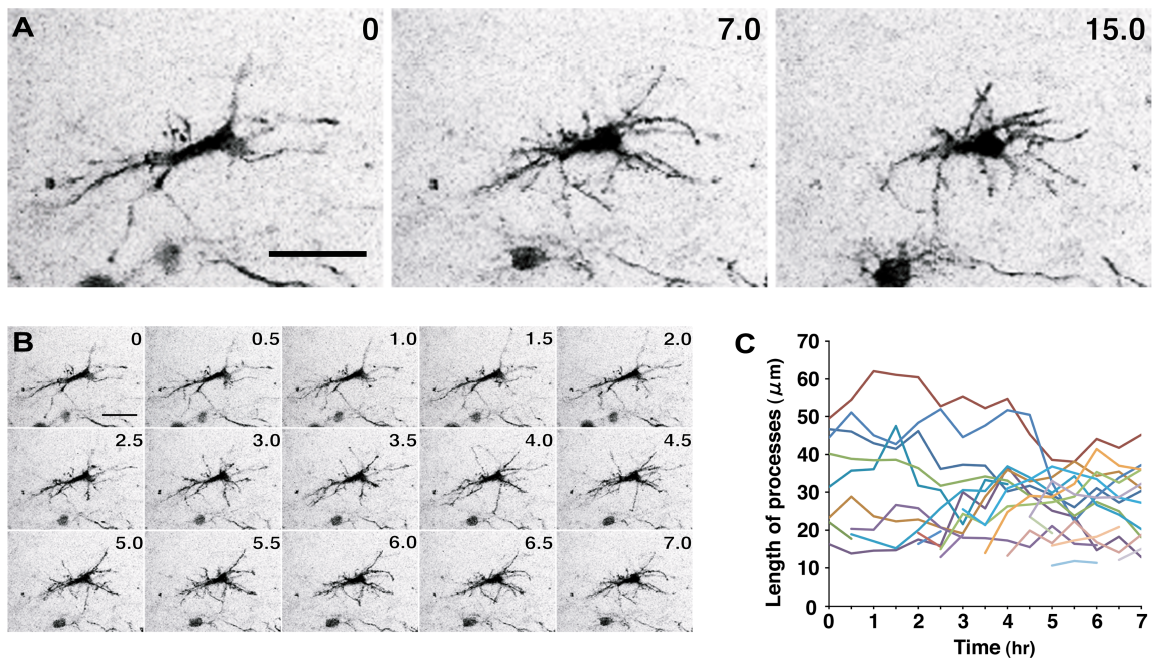


Figure 1. Sea urchin-like cells alternately extend and retract short processes.
 (A, B) Time sequence of confocal images of a sea urchin-like cell. Imaging began at P0.5. Elapsed time after start of observation (hr) is indicated on the upper right corner of each photograph. (C) Length of processes of cell shown in B plotted against elapsed time. Different colors represent different processes. Extensions and retractions can be seen. (D) Time course of the morphological change of labelled cells in the cortex. The rate of multipolar cells is shown in black line and that of bipolar cells in gray dotted line and that of migrating cells in gray line. Scale bar: 30 μ m

Elongation of an axon-like process

During the course of real-time imaging, I noted that, unlike most processes, which repeatedly extended and retracted, one process from the sea urchin-like cells continued to elongate during the period of observation or until it exited the observation field. Figure 2 A exemplifies such an extension. This neuron showed multiple processes extending and retracting for 7.5 h from the onset of observation (Fig. 2A ($t = 0$ - $t = 7.5$), B). However, suddenly one began to elongate almost monotonically up to the end of the observation period (Fig. 2A). The thin and long morphology of this process together with its distinct behavior from others strongly suggests that this is a prospective axon. Indeed, growth cone-like swellings were observed at the leading edge of such elongating processes (Fig. 2C-E). Such an extension of processes from labeled cells occurred in a widespread manner across the developing neocortex (Fig. 2G,H, magenta-colored neurons) (64 neurons in five brains). On some occasions, multiple long processes elongated to some extent. However, eventually only one exceeded a length of 200 μ m (Fig. 2F).

Axon-like processes appeared to preferentially extend radially (Fig. 2G,H, magenta-colored cells), with the majority toward the ventricle and a minority toward the pial surface. I analyzed the direction of the extension of the axon-like processes. The coronal plane was divided into four quadrants, and the direction was analyzed (Materials and Methods and Fig. 4). We found that a predominant population of labeled cells ($59.9\% \pm 12.8\%$) extended axon-like processes radially away from the pial surface ($n=41/64$ cells, 5 brains), whereas a minority ($21.1\% \pm 9.3\%$) extended toward the pial surface ($n=14/64$ cells, 5 brains).

Some sea urchin-like cells did not extend axon-like processes during the

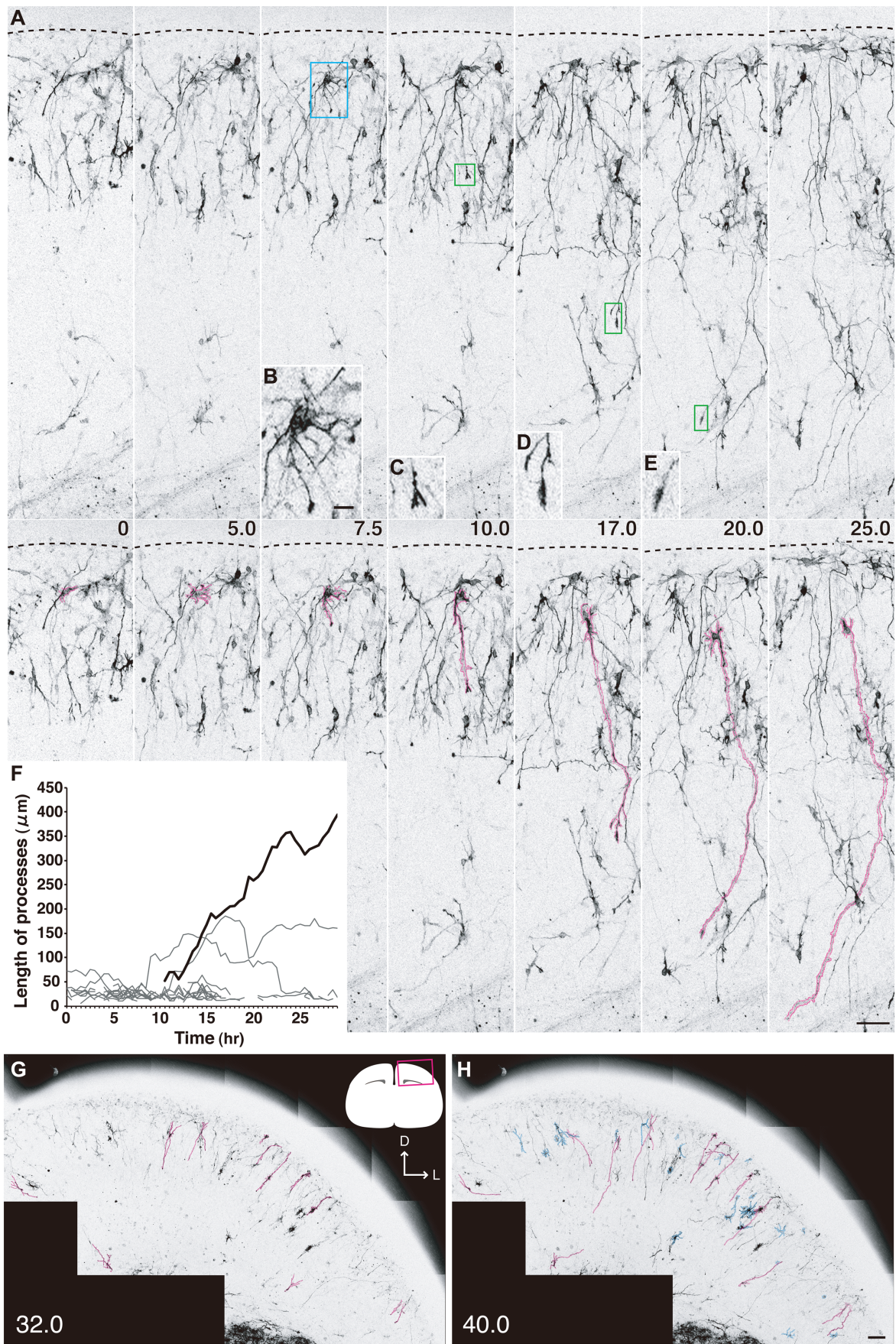
observation period. The fact that the initiation of axon-like processes occurred at different time points among different cells, however, suggests that those cells would also elongate axon-like processes but at a later developmental stage.

I also observed rapidly migrating cells among sea urchin-like cells, which are stationary. These migrating cells had leading processes, but the lengths of which never exceeded 200 μm , indicating that the rapidly extending process from sea urchin-like cells is distinct.

→

Figure 2. Extension of an axon-like process from a sea urchin-like cell.

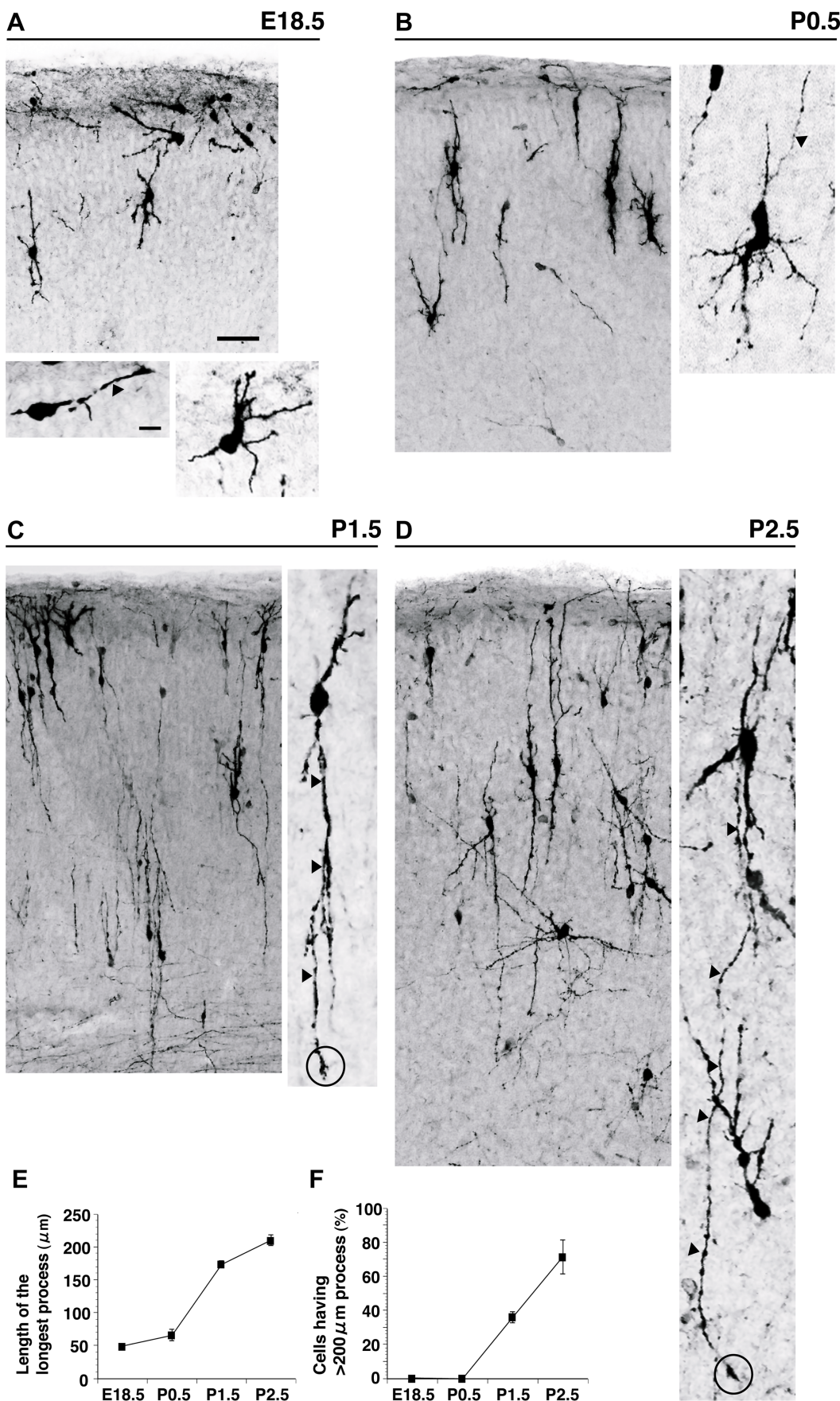
(A) Time sequence of confocal images of a cell that initiated an axon-like process during time-lapse imaging. Time-lapse imaging began at P0.5. Panels in upper and lower rows show the same cell, but in the lower row an axon-like process is marked in pink. Elapsed time after the onset of imaging (hr) is indicated on the upper right corner of the lower panels. Dashed lines indicate the pial surface. (B-E) Growing tips of axon-like processes. High magnification of the areas demarcated by rectangles in (A). B corresponds to the blue rectangle in (A) and shows a sea urchin like-cell that has just initiated an axon-like process headed by a growth cone. (C-E) Growing tips of the axon-like process demarcated by green rectangles in (A). (F) Time course of the extension of several processes from a sea urchin-like cell. Many short processes repeatedly extend and retract, but one continues to extend almost monotonically (thick black line). Note that two other processes extend up to 150-200 μm but fail to extend further. This cell corresponds to the one shown in Movie 4. (G,H) Low-magnification images of the lateral cortex showing the morphologies of interneurons extending axon-like processes (magenta). (G) Image taken 32 hr after the onset of imaging; (H) 40 hr. Comparison of these two images demonstrates extension of long processes. Scale bars: A, 30 μm ; B-E, 10 μm ; G, H, 100 μm . D, Dorsal; L, lateral.



In vivo preparations

The peculiar features of the sea urchin-like cells and extension of axon-like processes raise the question as to whether these are in vitro artifacts or not. To test this possibility, I examined the morphology of labeled cells in fixed preparations not been subjected to culture. Observation of labeled cells in the CP at late embryonic and early postnatal days revealed cells with a remarkably similar morphology to the observed sea urchin-like cells (Fig. 3 A, B), demonstrating that our results are not artifacts.

If the elongation of axon-like processes observed in the time-lapse imaging occurs in vivo, we should be able to observe an increase in the number of cells with axons in fixed brains. As expected, I found that a majority of labeled cells observed in preparations fixed at P1.5-P2.5 had one process significantly longer than the rest (Fig. 3C,D, arrowheads). Moreover, a growth cone-like protrusion was observed at the leading edge of such long processes (Fig. 3C,D, circle). Figure 3, E and F, shows developmental changes in the length of the longest process and the proportion of labeled neurons that had a process 200 μ m at each developmental stage. It should also be noted that both the length and proportion suddenly began to increase at P0.5, consistent with in vitro observations that found the initiation of the axonal growth takes place around this same stage.



←

Figure 3. GABAergic interneurons observed in perinatal mouse neocortex *in vivo*. Neurons in the CP and marginal zone are shown. A-D, Confocal images of samples fixed in coronal sections at E18.5 (A), P0.5 (B), P1.5 (C), and P2.5 (D). Most labeled cells in the marginal zone show migrating neurons with a bipolar shape (A, bottom left), but those in the CP primarily showed a multipolar morphology at E18.5 (A, bottom right). At P0.5, although labeled cells extend longer processes, many show multipolar morphology. At later stages, cellular morphologies become more complex (D). In A-D, the largest panel in each shows a low-magnification view of the representative samples. The bottom two panels in A and right panels in B-D show high-power pictures. E, Length of the longest process becomes larger as development proceeds. F, Proportion of labeled cells bearing a long (>200 μ m) process markedly increases during postnatal development. In E and F, numbers of neurons analyzed were 833 at E18.5, 745 at P0.5, 915 at P1.5, and 702 at P2.5. Scale bars: top panel in A, left panels in B-D, 50 μ m; bottom panels in A, right panels in B-D, 10 μ m.

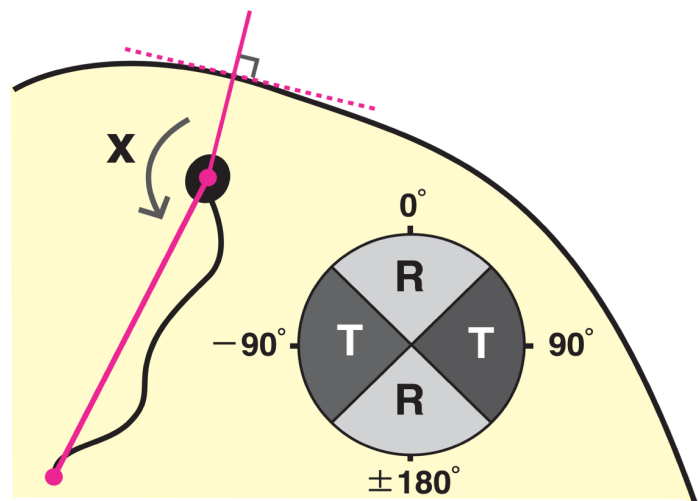


Figure 4. Schematic which indicates the method for measuring the orientation of axonal growth. The orientation was categorized into four quadrants, each being tangential (T) or radial (R). The radial was further divided into pia directed and ventricle directed. See Materials and Methods for detail.

These changes in the morphology of individual neurons occurred concomitant with changes in their orientation, from tangential to radial, and changes in the zonal distribution of labeled cells, from the MZ to the CP (Fig. 5), supporting the notion that extension of the axon-like process is related to the maturation of interneurons.

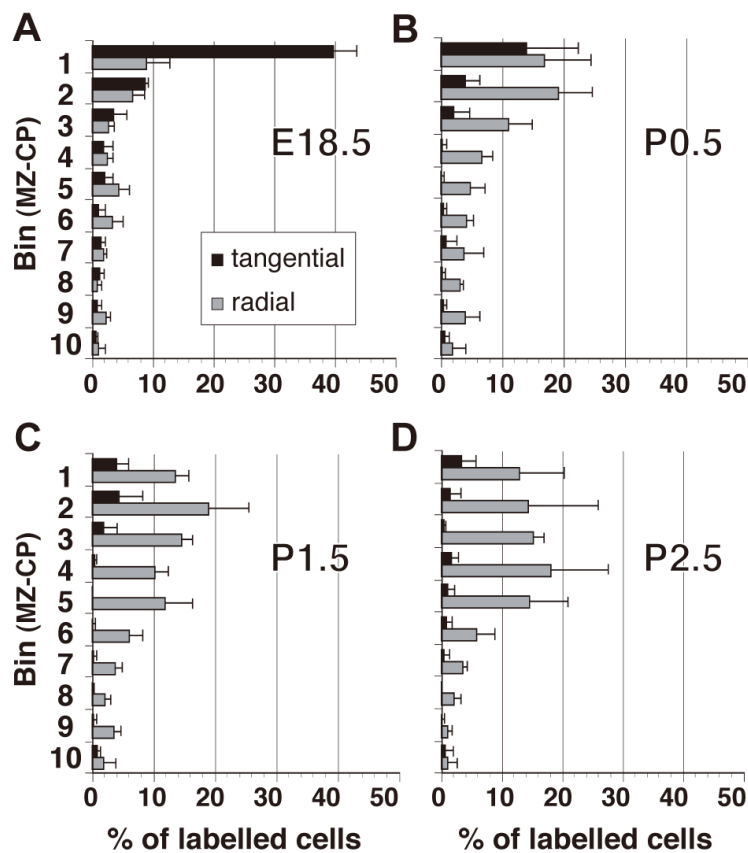


Figure 5. Changes in zonal distribution, orientation and morphology of cortical interneurons during perinatal development. (A-D) Zonal distribution of GABAergic interneurons in MZ-CP and the orientation of the longest processes. Interneurons labeled by electroporation at E12.5. Filled columns indicate tangentially oriented neurons and open columns indicate radially oriented neurons (see Figure S1). Cortical plate-marginal zone was divided into into 10 bins of equal thickness and progressive depth. Note, as development proceeds, tangentially oriented neurons decrease and a larger proportion of labeled neurons become situated in deeper zones. Distribution at four different stages is shown. $n = 4$ brains, 833 cells (E18.5), $n = 5$ brains, 745 cells (P0.5), $n = 3$ brains, 915 cells (P1.5), $n = 4$ brains, 702 cells (P2.5)

The labeled interneurons appeared to be a specific subset of interneurons, because they were primarily localized to specific layers, namely layers II/II and IV, when examined at P7. Interestingly, some of these cells looked like fast-spiking basket or double bouquet cells extending a vertically oriented axon (Fig. 6) (Uematsu et al., 2008). Immunostaining for PV, SST, or CR in P21 mice demonstrated that 60% of double-labeled cells expressed PV and 40% expressed either SST or CR (data not shown).

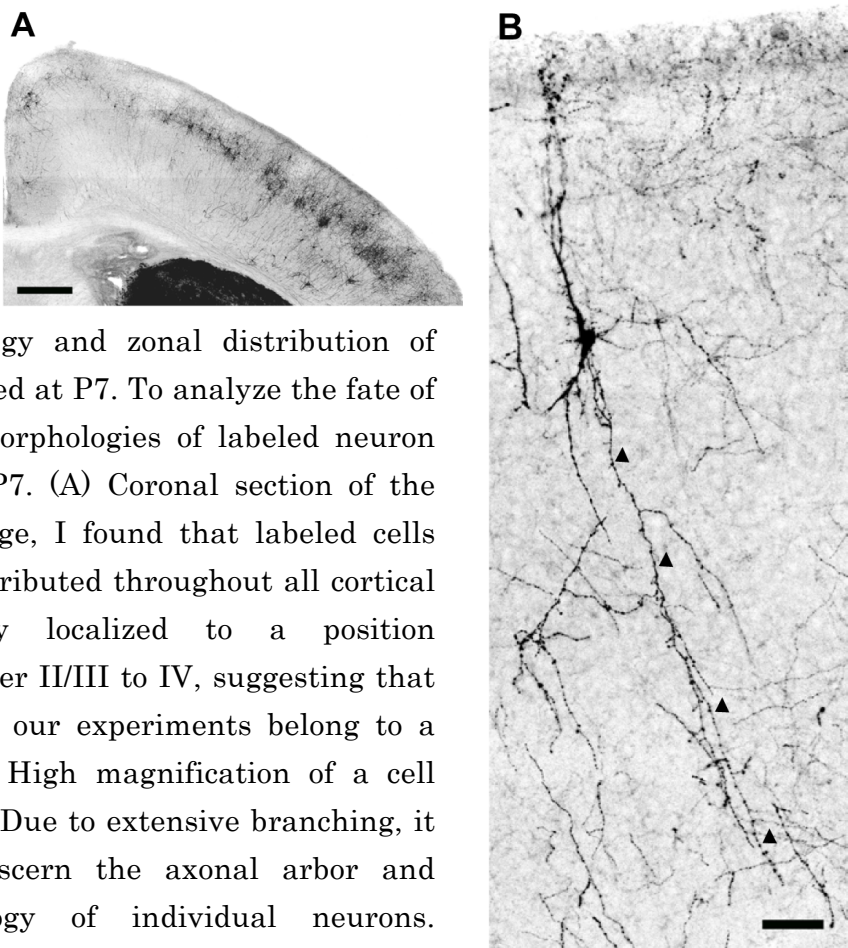


Figure 6. Morphology and zonal distribution of interneurons observed at P7. To analyze the fate of labeled processes morphologies of labeled neuron were examined at P7. (A) Coronal section of the cortex. At this stage, I found that labeled cells were not evenly distributed throughout all cortical layers but mostly localized to a position corresponding to layer II/III to IV, suggesting that the cells labeled by our experiments belong to a specific subset. (B) High magnification of a cell labeled in isolation. Due to extensive branching, it was difficult to discern the axonal arbor and dendritic morphology of individual neurons. Nevertheless, we found that some of the cells extended a long and vertically oriented non-tapering process (arrowheads) reminiscent of the morphologies of double bouquet or Martinotti cells (Uematsu et al., 2008), which extends a long vertically oriented axon. Scale bar: 500 μ m in A and 50 μ m in B.

Discussion

I have demonstrated that, during early postnatal development, cortical interneurons transiently exhibit sea urchin-like morphology, alternating between extended and retracted short processes, one of which suddenly elongated rapidly to transform into an axon-like morphology.

Sea urchin-like cells

I have demonstrated the occurrence of sea urchin-like interneurons in newborn mice cortex. Unlike migrating neurons observed at earlier stages (Nadarajah et al., 2002; Polleux et al., 2002; Tanaka et al., 2003, 2006, 2009), sea urchin-like cells alternately extend and retract many short processes without showing notable migration. It is unlikely that the sea urchin-like cell is an *in vitro* artifact because cells with similar morphologies were observed in fixed brains not subjected to culture (Fig. 3). The occurrence of neurons with similar morphologies in Golgi-impregnated preparations from kittens (Meyer and Ferres-Torres, 1984) supports this interpretation. Sea urchin-like cells remind us of multipolar cells reported in the embryonic cortex (Tabata and Nakajima, 2003) and cerebellar granule cells that settle in the inner granular layer (Kawaji et al., 2004). However, the former is distinct from sea urchin-like cells in that they are still in the course of migration. The latter also appears to be different in that they have a long axon-like leading process reaching the external granular layer, yet both have common features with our sea urchin-like cells and these two as all can completely or transiently cease migration. Therefore, one can surmise that neurons that stop migration, either

transiently or permanently, exhibit non-polarized morphologies and alternate between extending and retracting processes.

GABAergic interneurons are essentially bipolar in shape with a branched or unbranched leading process when they migrate in the subventricular zone and the MZ (Nadarajah et al., 2002; Polleux et al., 2002; Tanaka et al., 2003, 2006, 2009; Martini et al., 2009). These same neurons are likely to transform into sea urchin-like cells because the proportion of interneurons with a bipolar shape decrease during the perinatal stage in experiments in which interneurons were labeled at E12.5 (E.Y. and F.M., unpublished observation). Indeed, I occasionally observed the transformation of migrating GABAergic interneurons with a simple morphology into sea urchin-like cells.

Initiation of axons

After taking the sea urchin-like shape, cortical interneurons initiate thin, long processes. It is highly likely that these processes are prospective axons because (1) they continue to elongate while other processes repeat retractions and extensions, (2) they are headed by highly motile, growth cone-like swellings during elongation, (3) they are significantly longer than other processes, (4) they do not taper off at their ends, and (5) they are longer than the leading processes of rapidly migrating neurons observed in the same preparation. In addition, the orientations of the prospective axon processes are similar to those of cortical interneuron subsets in the mature cortex such as fast-spiking basket, double bouquet, calretinin horizontal/descending arbor, and somatostatin cells (Uematsu et al., 2008).

Analysis of fixed samples further supports our interpretation. In fixed

preparations, I observed labeled neurons with morphologies similar to those described above, and the length of the longest process increased during early postnatal development. Some of such a processes expressed an axonal marker (Fig. 7). Furthermore, my preliminary experiments in which the morphologies of labeled cells were analyzed at a later stage, P7, I found neurons with vertically oriented axons reminiscent of double bouquet (Fig. 6).

Together, the initiation of axons from interneurons likely occurs after cortical interneurons become sea urchin-like cells. However, I cannot unequivocally rule out the possibility that the long processes I observed eventually retract and that new processes emerge during a later stage.

In fixed samples, I observed a minor proportion of neurons whose axons extended toward the pial surface, some of which even reached marginal zone. Therefore, it is possible that, for these cells, the trailing process turns into the axon.

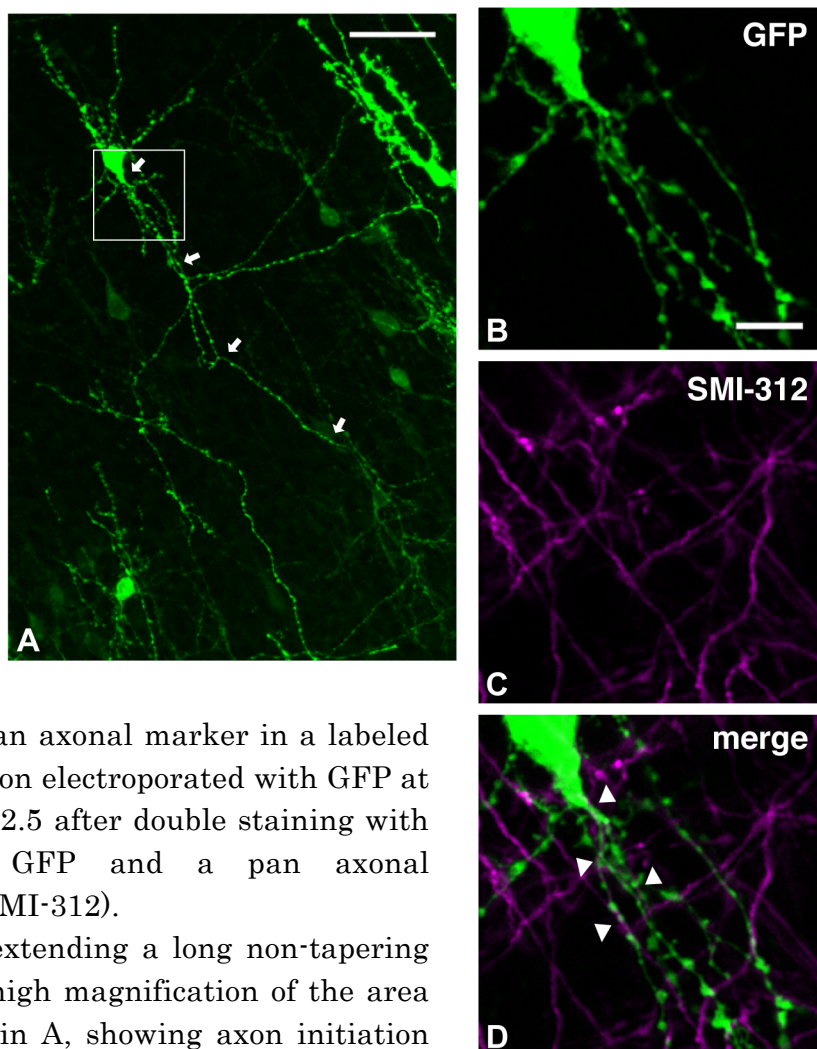


Figure 7. Expression of an axonal marker in a labeled interneuron. A interneuron electroporated with GFP at E12.5 was observed at P2.5 after double staining with an antibody against GFP and a pan axonal neurofilament marker (SMI-312).

(A) A GFP-labeled cell extending a long non-tapering process (arrows). (B) A high magnification of the area depicted by a rectangle in A, showing axon initiation site of a GFP-labeled interneuron. (C) SMI-312 immunoreactivity of the same section. (D) Merged view. Note that a thin axonal profile is double labeled (arrowheads). Scale bar: 50 μ m in A and 10 μ m in B-D.

Direction and orientation of axonal growth

The reason the axons preferentially elongate either toward or away from the pial surface remains unknown. One possibility is environmental attractive cues. In *Caenorhabditis elegans*, a diffusible axon guidance molecule, UNC-6, induces ventrally directed polarity in neurons (Adler et al., 2006).

Likewise, a secreted molecule, semaphorin 3A, regulates the axon-dendritic polarity in cortical pyramidal neurons *in vitro* (Polleux et al., 1998, 2000). It is possible that a similar mechanism determines the direction of axonal extensions seen in my study. However, I cannot preclude the possibility that interneurons have predetermined but morphologically undetectable polarity before initiation of axons.

Axonal growth from interneurons most often occurred along the radial axis in a very strict manner. Although the reason for this stereotyped orientation of growth remains unknown, it is possible that the axons use some physical substrate for their growth. Potential candidates include radial glial fibers and apical dendrites from excitatory neurons, because these processes strictly extend along the radial axis.

My results are consistent with those from classic experiments done by Dotti and colleagues (1988) in which neurons exhibited a non-polarized shape before the initiation of the axon. Given that many processes extend and retract before the axonogenesis (Fig. 2F) and multiple processes extend on either the basal or apical side and that I found multiple axon-like processes elongated and retracted alternately until one unexpectedly became an axon-like process, it is likely that axonal fate of cortical interneurons is determined stochastically (Bradke and Dotti, 2000).

In this study, I show that, during perinatal development, cortical interneurons initiate an axon from a morphologically non-polarized shape concurrently with changes in zonal distribution from the MZ to the CP (Fig. 8). This mode of axon initiation may be a widely occurring phenomenon but was first illustrated here using long-term live imaging of a cortical explant.

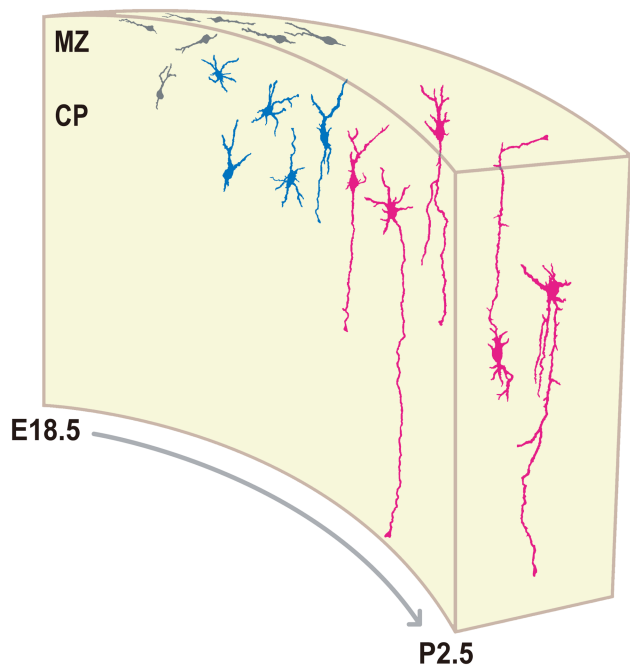


Figure 8. Schematic showing transitions of cortical interneuron morphology during perinatal development. Most cortical interneurons labeled by electroporation tangentially migrated in the MZ at E18.5. At this stage, they showed morphologies typical for migrating neurons extending a leading and a trailing process (gray). As development proceeds, they become situated in the CP, in which many of them alternately extend and retract of short processes (blue). These cells had a low motility of somata. Some of these cells then began to extend a long axon-like process (magenta) primarily toward the ventricle.

References

Adler CE, Fetter RD, Bargmann CI (2006) UNC-6/Netrin induces neuronal asymmetry and defines the site of axon formation. *Nat Neurosci*. 9:511-518.

Anderson SA, Eisenstat DD, Shi L, Rubenstein JL (1997) Interneuron migration from basal forebrain to neocortex: dependence on Dlx genes. *Science*. 278:474-476.

Arimura N, Kaibuchi K (2007) Abstract Neuronalpolarity: from extracellular signals to intracellular mechanisms. *Nat Rev Neurosci* 8:194 –205.

Bortone D, Polleux F (2009) KCC2 expression promotes the termination of cortical interneuron migration in a voltage-sensitive calcium-dependent manner. *Neuron* 62:53-71.

Bradke F, Dotti CG (2000) Establishment of neuronal polarity: lessons from cultured hippocampal neurons. *Curr Opin Neurobiol* 10:574-581.

Dotti CG, Sullivan CA, Banker GA (1988) The establishment of polarity by hippocampal neurons in culture. *J Neurosci*. 8:1454-1468.

Goslin K, Banker G (1989) Experimental observations on the development of polarity by hippocampal neurons in culture. *J Cell Biol* 108:1507–1516.

Hinds JW, Hinds PL (1974) Early ganglion cell differentiation in the mouse retina: an electron microscopic analysis utilizing serial sections. *Dev Biol*. 37:381-341.

Hinds JW, Hinds PL (1978) Early development of amacrine cells in the mouse retina: An electron microscopic, serial section analysis. *J Comp Neurol*. 179:277-300.

Kawaji K, Umeshima H, Eiraku M, Hirano T, Kengaku M (2004) Dual phases of migration of cerebellar granule cells guided by axonal and dendritic leading processes. *Mol Cell Neurosci*. 25:228-240.

Lambert de Rouvroit C, Goffinet AM (2001) Neuronal migration. *Mech Dev*. 105:47-56.

Lavdas AA, Grigoriou M, Pachnis V, Parnavelas JG (1999) The medial ganglionic eminence gives rise to a population of early neurons in the developing cerebral cortex. *J. Neurosci*. 19:7881-7888.

Martínez S, Puelles L, Alvarado-Mallart RM (1992) Tangential neuronal migration in the avian tectum: cell type identification and mapping of regional differences with quail/chick homotopic transplants. *Brain Res Dev Brain Res*. 66:153-163.

Martini FJ, Valiente M, López Bendito G, Szabó G, Moya F, Valdeolmillos M, Marín O (2009) Biased selection of leading process branches mediates chemotaxis during tangential neuronal migration. *Development*. 136:41-50.

Meyer G, Ferres-Torres R (1984) Postnatal maturation of nonpyramidal neurons in the visual cortex of the cat. *J Comp Neurol* 228:226 -244.

Nadarajah B, Alifragis P, Wong RO, Parnavelas JG (2002) Ventricle-directed migration in the developing cerebral cortex. *Nat Neurosci* 5:218 -224.

Polleux F, Morrow T, Ghosh A (2000) Semaphorin 3A is a chemoattractant for cortical apical dendrites. *Nature*. 404:567-573.

Polleux F, Giger RJ, Ginty DD, Kolodkin AL, Ghosh A (1998) Patterning of cortical efferent projections by semaphorin-neuropilin interactions. *Science*. 282:1904-1906.

Polleux F, Whitford KL, Dijkhuizen PA, Vitalis T, Ghosh A (2002) Control of cortical interneuron migration by neurotrophins and PI3-kinase signaling. *Development* 129:3147-3160.

Stensaas LJ (1967a) The development of hippocampal and dorsolateral pallial regions of the cerebral hemisphere in fetal rabbits. I. Fifteen millimeter stage, spongioblast morphology. *J Comp Neurol*. 129:59-69.

Stensaas LJ (1967b) The development of hippocampal and dorsolateral pallial regions of the cerebral hemisphere in fetal rabbits. II. Twenty millimeter stage, neuroblast morphology. *J Comp Neurol*. 129:71-83.

Tabata H, Nakajima K (2003) Multipolar migration: the third mode of radial neuronal migration in the developing cerebral cortex. *J Neurosci* 23:9996-10001.

Tamamaki N, Fujimori KE, Takaaji R (1997) Origin and route of tangentially migrating neurons in the developing neocortical intermediate zone. *J Neurosci* 17:8313-8323.

Tamamaki N, Yanagawa Y, Tomioka R, Miyazaki J, Obata K, Kaneko T (2003) Green fluorescent protein expression and colocalization with calretinin, parvalbumin, and somatostatin in the GAD67-GFP knock-in mouse. *J Comp Neurol* 467:60-79.

Tanaka DH, Maekawa K, Yanagawa Y, Obata K, Murakami F (2006) Multidirectional and multizonal tangential migration of GABAergic interneurons in the developing cerebral cortex. *Development* 133:2167-2176.

Tanaka D, Nakaya Y, Yanagawa Y, Obata K, Murakami F (2003) Multimodal tangential migration of neocortical GABAergic neurons independent of GPI-anchored proteins. *Development* 130:5803-5813.

Tanaka DH, Yanagida M, Zhu Y, Mikami S, Nagasawa T, Miyazaki J, Yanagawa Y, Obata K and Murakami F (2009) Random walk behavior of migrating cortical interneurons in the marginal zone: time-lapse analysis in flat-mount cortex. *J. Neurosci.* 29:1300-1311.

Tsai LH, Gleeson JG (2005) Nucleokinesis in neuronal migration. *Neuron* 46:383-388.

Uematsu M, Hirai Y, Karube F, Ebihara S, Kato M, Abe K, Obata K, Yoshida S, Hirabayashi M, Yanagawa Y, Kawaguchi Y (2008) Quantitative chemical composition of cortical GABAergic neurons revealed in transgenic venus-expressing rats. *Cereb Cortex* 18:315-330.

Wentworth LE, Hinds JW (1978) Early motoneuron formation in the cervical spinal cord of the mouse: an electron microscopic, serial section analysis. *J Comp Neurol.* 177:611-613.

Wilcock AC, Swedlow JR, Storey KG (2007) Mitotic spindle orientation distinguishes stem cell and terminal modes of neuron production in the early spinal cord. *Development*. 134:1943-1954.

General discussion

I have carried out real-time imaging of axon formation from sea urchin-like GABAergic interneurons in *in vivo*-like culture tissue for the first time. During migration, GABAergic interneurons exhibited bipolar shape. However, they began to exhibit multipolar shape in the CP of the cerebral cortex. They suddenly extended a long axon-like process repeating extension and retraction of short processes. Many imaging experiments have been carried out previously, but those previous studies did not observe the process of axonal formation and elongation in *in vivo*-like preparations as was used in my study (for review, see Hatanaka et al., 2012).

A different pattern of axonal formation in neuronal development has been reported in retinal ganglion cells (RGCs). Thus, it was suggested that axonal elongation from sea urchin-like cells is not observed in general. Electron microscopic observations of serial thin sections (Hinds and Hinds, 1974) indicated that axonal extensions from RGCs occur from basal processes that contact the inner limiting membrane of the neuroepithelium. The description of axonal extensions from RGCs was confirmed by real-time imaging (Zolessi et al., 2006). They monitored differentiating RGCs in which the apical process was clearly visible by using four-dimensional microscopy of developing RGCs in live zebrafish embryos and demonstrated that the axon-like process emerges from a basal process of radially oriented immature neurons. Time-lapse imaging of the Kif5c560-YFP signal which selectively accumulates in axons (Nakata and Hirokawa, 2003; Jacobson et al. 2006; Konishi and Setou, 2009) in zebrafish RGCs confirmed the axonal nature of the process extended from the basal

process of the neuroepithelial cells (Randlett et al., 2011). Those findings indicated that axons of RGCs emerge from polarized neuroepithelial cells. However, as GABAergic interneurons tangentially migrate into the cerebral cortex and perform the multidirectional migration, they lose the radial polarity to the ventricle like as neuroepithelial progenitors. Therefore, they can't retain the polarity of neuroepithelial progenitors. Because of the differences in migration, the axonal formation of GABAergic interneurons may be different from that of RGCs.

Neuronal polarization and axon specification are necessary for axonal elongation. Neuronal polarization in vitro is directed by asymmetric presentation of Netrin1 (known as UNC-6 in *C.elegans*), BDNF, TGF- β , cAMP/cGFP, or Sema3a, or by contact with cell adhesion or extracellular matrix molecules (Esch et al., 1999; Gupta et al., 2010; Mai et al., 2009; Me'nager et al., 2004; Polleux et al., 1998; Shelly et al., 2007). The orientation of axon-like processes elongated from sea urchin-like cells was almost radial and so it is possible that those extracellular molecules localized to the ventricle and the pia attract an axon in the cortex. Moreover, radial glial fibers and apical dendrites from excitatory neurons may support for the stereotyped orientation. For axon specification and the establishment of neuronal polarity, a differential regulation of actin and microtubule cytoskeleton dynamics at the growth cones of the developing neuritis in a polarizing neuron is critical (Bradke and Dotti, 1999; Stiess and Bradke, 2011; Witte and Bradke, 2008; Witte et al., 2008). Therefore, I propose the direction of axonal elongation depends on neuronal polarity directed by extracellular molecules and above-mentioned physical substrates and actin and microtubule cytoskeleton dynamics at the growth cone of pre-axon in sea urchin-like cells are regulated to form an axon along the

directed polarity. Because the timing of the elongation of axon-like processes were various in a tissue preparation in my study, it is suggested that the reactivity to extracellular molecules for axonal elongation is regulated in different cells in the cortex. Moreover, excitatory cortical neurons with multipolar shapes extend an axon that is perpendicular to the ventricle like as GABAergic interneurons (Hatanaka and Yamauchi, 2012) and so they may have the same mechanism for axonal formation.

To elucidate the mechanism for axonal elongation in sea urchin-like cells, the real-time imaging of the dynamics of intracellular proteins and organelle in axonal elongation from sea urchin-like cells are required. The method of real-time imaging in my study is suited to gain the results with in vivo-like condition for the purpose. Recently, real-time imaging experiments have been carried out using living mouse embryos to observe neuronal migration (Inada et al., 2011; Scott et al., 2012; Yanagida et al., 2012). Although such experiments require sophisticated techniques, observations of axon elongation in such in vivo conditions should be required to uncover genuine axon initiating behaviors from developing neurons.

Note that, our results give an important suggestion to the neuronal maturation. I indicated that sea urchin-like neurons began to elongate an axon-like process at the early stage of neuronal maturation. The presences of sea urchin-like neurons that elongate an axon provide an important insight into neuronal maturation for the formation of neuronal circuit.

References for general discussion

Bradke F, Dotti CG (1999) The role of local actin instability in axon formation. *Science* 283, 1931-1934.

Esch T, Lemmon V, Banker G (1999) Local presentation of substrate molecules directs axon specification by cultured hippocampal neurons. *J. Neurosci.* 19, 6417-6426.

Gupta SK, Meiri KF, Mahfooz K, Bharti U, Mani S (2010) Coordination between extrinsic extracellular matrix cues and intrinsic responses to orient the centrosome in polarizing cerebellar granule neurons. *J. Neurosci.* 30, 2755-2766.

Hatanaka Y, Yamauchi K (2012) Excitatory cortical neurons with multipolar shape establish neuronal polarity by forming a tangentially oriented axon in the intermediate zone. *Cereb Cortex* 23(1):105-13.

Hatanaka Y, Yamauchi K, Murakami F (2012) Formation of axon-dendrite polarity in situ: initiation of axons from polarized and non-polarized cells. *Dev Growth Differ.* 54(3):398-407.

Hinds JW, Hinds PL (1974) Early ganglion cell differentiation in the mouse retina: an electron microscopic analysis utilizing serial sections. *Dev Biol.* 37:381-341.

Inada H, Watanabe M, Uchida T, Ishibashi H, Wake H, Nemoto T, Yanagawa Y, Fukuda A, Nabekura J (2011) GABA regulates the multidirectional tangential migration of GABAergic interneurons in living neonatal mice. *PLoS One.* 6(12).

Jacobson C, Schnapp B, Banker GA (2006) A change in the selective translocation of the Kinesin-1 motor domain marks the initial specification of

the axon. *Neuron* 49, 797-804.

Konishi Y, Setou M (2009) Tubulin tyrosination navigates the kinesin-1 motor domain to axons. *Nat. Neurosci.* 12, 559-567.

Mai J, Fok L, Gao H, Zhang X, Poo MM (2009) Axon initiation and growth cone turning on bound protein gradients. *J. Neurosci.* 29, 7450-7458.

Me' nager C, Arimura N, Fukata Y, Kaibuchi K (2004) PIP3 is involved in neuronal polarization and axon formation. *J. Neurochem.* 89, 109-118.

Nakata T, Hirokawa N (2003) Microtubules provide directional cues for polarized axonal transport through interaction with kinesin motor head. *J. Cell Biol.* 162, 1045-1055.

Polleux F, Giger RJ, Ginty DD, Kolodkin AL, Ghosh, A. (1998) Patterning of cortical efferent projections by semaphorin-neuropilin interactions. *Science* 282, 1904-1906.

Randlett O, Poggi L, Zollessi FR, Harris WA (2011) The oriented emergence of axons from retinal ganglion cells is directed by laminin contact in vivo. *Neuron* 70, 266-280.

Scott BB, Gardner T, Ji N, Fee MS, Lois C (2012) Wandering neuronal migration in the postnatal vertebrate forebrain. *J Neurosci.* 25;32(4):1436-46.

Shelly M, Cancedda L, Heilshorn S, Sumbre G, Poo MM (2007) LKB1/STRAD promotes axon initiation during neuronal polarization. *Cell* 129, 565-577.

Stiess M, Bradke F (2011) Neuronal polarization: the cytoskeleton leads the way. *Dev. Neurobiol.* 71, 430-444.

Witte H, Bradke F (2008) The role of the cytoskeleton during neuronal

polarization. *Curr. Opin. Neurobiol.* 18, 479-487.

Witte H, Neukirchen D, Bradke F (2008) Microtubule stabilization specifies initial neuronal polarization. *J. Cell Biol.* 180, 619-632.

Yanagida M, Miyoshi R, Toyokuni R, Zhu Y, Murakami F (2012) Dynamics of the leading process, nucleus, and Golgi apparatus of migrating cortical interneurons in living mouse embryos. *Proc Natl Acad Sci U S A.* 109(41):16737-42.

Zolessi FR, Poggi L, Wilkinson CJ, Chien CB, Harris WA (2006) Polarization and orientation of retinal ganglion cells in vivo. *Neural. Dev.* 1, 2.

Acknowledgement

I thank Dr. D. Tanaka-Harada for technical advice and generous support, T. Kobayashi for *pCAGGS-GAP-EGFP*, Dr. Y. Hatanaka for *pCAG-EGFP* and *pCAG-dsRed2*, Dr. F. Murakami for critically reading this manuscript. Finally, I also thank all the Murakami laboratory members for their support and input on this work.

Bibliography

[Original article]

Yamasaki E, Tanaka DH, Yanagawa Y and Murakami F. (2010) Cortical GABAergic Interneurons Transiently Assume a Sea Urchin-like Non-polarized Shape Prior to Axon Initiation. *J. Neurosci.* 30(45), 15221-15227

[Review]

Murakami F, Tanaka D, Yanagida M and Yamazaki E. (2007) Intracortical multidirectional migration of cortical interneurons, CORTICAL DEVELOPMENT: GENES AND GENETIC ABNORMALITIES, Novartis Found Symp 288, 116-25; discussion 125-9, 276-81.

[Presentations]

Yamasaki E, Tanaka DH, Yanagawa Y, Obata K and Murakami F. Early steps of morphological maturation of neurons after termination of migration, 2007 Annual Meeting of the Molecular Biology Society of Japan & the Japanese Biochemical Society. Yokohama, Japan (Poster & Talk) (2007)

Yamasaki E, Tanaka DH, Yanagawa Y, Obata K and Murakami F. Early steps of morphological maturation of neurons after termination of migration, 第2回神経発生討論会 Okazaki, Japan (Talk) (2008)